J Electr Eng Technol.2018; 13(6): 2402-2411
http://doi.org/10.5370/JEET.2018.13.6.2402

ISSN(Print) 1975-0102
ISSN(Online) 2093-7423

Analysis on Temperature Distribution and Current-Carrying Capacity of GIL Filled with Fluoronitriles-CO_2 Gas Mixture

Geng Chen*, Youping Tu*, Cong Wang†, Yi Cheng*, Han Jiang*, Hongyang Zhou* and Hua Jin**

Abstract – Fluoronitriles-CO_2 gas mixtures are promising alternatives to SF_6 in environmentally-friendly gas-insulated transmission lines (GILs). Insulating gas heat transfer characteristics are of major significance for the current-carrying capacity design and operational state monitoring of GILs. In this paper, a three-dimensional calculation model was established for a GIL using the thermal-fluid coupled finite element method. The calculated results showed close agreement with experimentally measured data. The temperature distribution of a GIL filled with the Fluoronitriles-CO_2 mixture was obtained and compared with those of GILs filled with CO_2 and SF_6. Furthermore, the effects of the mixture ratio of the component gases and the gas pressure on the temperature rise and current-carrying capacity of the GIL were analyzed. Results indicated that the heat transfer performance of the Fluoronitriles-CO_2 gas mixture was better than that of CO_2 but worse than that of SF_6. When compared with SF_6, use of the Fluoronitriles-CO_2 gas mixture caused a reduction in the GIL's current-carrying capacity. In addition, increasing the Fluoronitriles gas component ratio or increasing the pressure of the insulating gas mixture could improve the heat dissipation and current-carrying capacity of the GIL. These research results can be used to design environmentally-friendly GILs containing Fluoronitriles-CO_2 gas mixtures.

Keywords: Gas-insulated transmission line, Fluoronitriles-CO_2 gas mixture, Thermal field calculation, Current-carrying capacity.

1. Introduction

The gas insulated transmission line (GIL) offers several advantages, which include high transmission capacity, reduced land occupation, good environmental compatibility and high operational reliability, and is particularly suitable for use in complex geographical environments, including high altitude conditions with large drops. In general, the GIL provides an effective alternative means of power transmission [1, 2]. The current-carrying capacity of the GIL is limited by its maximum temperature rise [3]. Because of its good closure performance and finite volume, an obvious heating phenomenon will occur in a GIL. The associated temperature rise not only reduces the maximum current-carrying capacity of the conductor, but also affects the performance of the insulation material and reduces the service life of the equipment [3, 4].

In recent years, to solve the serious greenhouse effect problems caused by SF_6, the 3M™ Company developed and commercialized a new fluoronitrile compound called 3M™ Novec™ 4710 Insulating Gas. Alstom Grid (GE) also proposed a new type of insulating gas called G3™, which is a Fluoronitriles-CO_2 mixture [5-7]. These changes in the type of gas will affect the heat dissipation properties of GILs; it is thus important to study the temperature distribution and the factors influencing the temperature rises in the GILs in which these new types of insulating gases are used.

The temperature rise effect in GILs can be determined via experimental testing and numerical calculations. However, a GIL will be affected by its operating state and by various environmental factors in its actual operation process. Only a finite number of temperature detection points can be obtained during experimental testing; however, the state of the fluid during operation and the overall operational aspects of the GIL cannot be determined because of the nonlinear relationship between the physical parameters of the fluid and the temperature. A coupling analysis of the electromagnetic field, the thermal field and the fluid field performed using numerical calculation methods can be used to solve the nonlinear problem for the physical parameters of the fluid [8, 9]. Common numerical calculation methods used in this field include the analytical method and the finite element method. The analytical method is generally used for the approximate initial calculation of the steady state temperature rise,

† Corresponding Author: Beijing Key Laboratory of High Voltage & EMC, North China Electric Power University, China. (cong@ncepu.edu.cn).
* State Key Laboratory of Alternate Electrical Power System with Renewable Energy Sources, North China Electric Power University, Beijing, China. (gengchenncepu@sina.com, typ@ncepu.edu.cn, {ncepu_cy, jianghan729912} @163.com).
** School of Control and Computer Engineering, North China Electric Power University, China. (jh@ncepu.edu.cn)
Received: February 26, 2018; Accepted: April 25, 2018

which is solved using an iterative solution by establishing the heat balance relationship in the GIL. However, only the average temperatures of the conductor and the enclosure can be obtained in this way. The finite element method can be used to simulate the state of the fluid during operation of the GIL through coupling of the electromagnetic field with the thermal-fluid field and allows the overall temperature distribution of the GIL to be obtained. In [10], the heat transfer characteristics of GILs in different external environments with different placement angles and different surface emissivities were analyzed using analytical methods and testing. In [11-14], the finite element method was used to perform two-dimensional temperature rise simulations of GILs containing SF_6, but mixed gases were not considered. The temperature rise of a second generation GIL using mixed SF_6-N_2 gas was simulated in [15] and the effects of the ratio of the component gases and the pressure on the temperature rise were analyzed. In [6] and [7], the heat transfer characteristics of Fluoronitriles-CO_2 gas mixtures were investigated experimentally, and the experimental results showed that the addition of low-concentration Fluoronitriles gas produced results that were obviously different from those obtained using pure CO_2. However, calculations of the temperature distribution of a GIL containing a Fluoronitriles-CO_2 gas mixture and its effects on the current-carrying capacity of the GIL have rarely been studied.

In this paper, the finite element method is used to simulate the temperature rise behavior of a vertically installed GIL containing mixed Fluoronitriles-CO_2 gas; the temperature distribution of this GIL is obtained, and design factors related to the GIL's temperature rise and its current-carrying capacity are analyzed. The research results reported here can serve as a theoretical basis for the design and application of environmentally-friendly GILs.

2. Simulation Model

The simulation model is established on the basis of a simplified GIL that has been installed vertically. The solution domain includes the external air around the GIL, the insulating gas, the metal conductor and the metal enclosure. The geometric model is shown in Fig. 1.

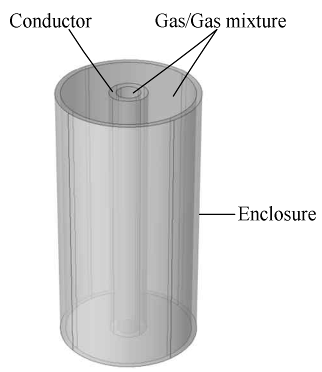

Fig. 1. Geometric model of the GIL

2.1. Electromagnetic field

The heat losses related to the Joule effect in the conductor and the enclosure are obtained via calculation of the steady-state electromagnetic field. In this calculation, the influence of the displacement current is neglected and the vector magnetic potential A is used. When current flows in the GIL conductor, an eddy current is induced in the enclosure. Therefore, the Joule heating loss of the GIL consists of two parts and includes the current loss in the conductor and the eddy current loss in the enclosure. The governing equation is given as follows [13]:

$$\nabla \times \nu\left(\nabla \times A\right) = J_s + J_e = J_s - \sigma_e \frac{\partial A}{\partial t} \tag{1}$$

where ν is the reluctivity of the material, J_s and J_e represent the source current and the vector of the eddy current density, respectively, and e is the conductivity of the material.

When the influence of the temperature on the material resistivity is considered, the Joule heat loss Q_r per unit length in the conductor and the enclosure of the GIL can be expressed as follows.

$$Q_r = \int \rho(T) J^2 dS \tag{2}$$

$$\rho(T) = \rho_{293.15}\left[1 + \alpha_{293.15}(T - 293.15)\right] \tag{3}$$

where $\rho(T)$ is the resistivity of the material, J is the current density, $\rho_{293.15}$ represents the resistivity of the material at 293.15 K, $\alpha_{293.15}$ is the temperature coefficient of resistance at 293.15 K, and T is the thermodynamic temperature.

In engineering applications, the GIL conductor is usually made from aluminum, while the enclosure is usually made from an aluminum alloy. The characteristics and the size parameters of the GIL conductor and enclosure used in this paper are shown in Table 1 below.

2.2 Thermal-fluid coupled field

The GIL is a coaxial cylindrical system. Thermal convection and radiation remove the Joule heat losses from the conductor to the enclosure [11]. In addition to its own Joule heat losses, the enclosure also accepts the heat from the conductor. This heat is transferred to the surrounding environment via radiation and natural convection when the

Table 1. Material and dimensional parameters of the GIL

	External diameter (mm)	Thickness (mm)	$\rho_{293.15}$ ($10^{-8}\Omega\cdot m$)	$\alpha_{293.15}$ (1/K)
conductor	70	13	2.8	0.0039
enclosure	260	5	3.5	0.0040

GIL is thermally stable. In the interior structure composed of the conductor and the enclosure, heat is mainly transmitted by thermal conduction.

The calculation of the thermal field is based on the following assumptions.

1) The effects of wind speed and solar radiation on the temperature rise of the GIL are neglected.

2) The effects of small components on the thermal field, e.g., the pressure meter and the connecting bolts passing between the different parts of the enclosure, can be ignored.

3) The upper and lower sides of the GIL unit are separated using basin insulators with gas chambers contained in other units. The main insulator material is epoxy resin, which has a thermal conductivity that is much lower than that of the metal components. During actual operation, the heat exchange between the gas chambers in the different units is low, and the heat from the conductor is mainly lost through the enclosure. Therefore, the basin insulator can be simplified in this model and the two sides of the cavity are assumed to be adiabatic with the other gas chambers.

For the conjugate heat transfer problem, which is composed of linear combinations of various physical parameters, the multiple species transport model is used to solve for the fluid field using a single momentum conservation differential equation [14-16].

$$c_m=\sum_{i=1}^{n} X_i c_i \tag{4}$$

$$\sum_{i=1}^{n} X_i=1 \tag{5}$$

In the formula, c_i is the fluid density, thermal conductivity or dynamic viscosity of each component. X_i represents the mass fraction of each component. c_m is the complete physical parameter that corresponds to c_i, and n is the component fraction.

Based on the assumption that each component gas is an ideal gas, the density, the thermal conductivity and the dynamic viscosity are all functions of temperature. The specific heat is a fixed value and the physical properties can be determined using the following methods. The relationship between the density, the pressure and the temperature satisfies the ideal gas equation [17]

$$\rho_m=\rho_0 \frac{P}{T_0}\frac{S}{T} \tag{6}$$

The thermal conductivity (k) and the dynamic viscosity (μ) satisfy Sutherland's law of viscosity.

$$k_m = k_0 (\frac{T}{T_0})^{1.5} \frac{T_0+S}{T+S} \tag{7}$$

$$\mu_m=\mu_0 (\frac{T}{T_0})^{1.5} \frac{T_0+S}{T+S} \tag{8}$$

where ρ_0, k_0 and μ_0 are the density, thermal conductivity and dynamic viscosity of the Fluoronitriles or the CO_2 at room temperature. P is the gas pressure, and S is a fixed value related to the type of gas used at room temperature.

Because of the vertical installation of the GIL, the gas density will have an uneven distribution in the case where a heat source is used to heat a closed chamber, so a compressible laminar flow model with low Maher number was chosen. The governing equations include the equations of mass, momentum and energy conservation, which are given as follows.

$$\frac{\partial \rho}{\partial t}+\nabla\cdot\left(\rho u\right)=0 \tag{9}$$

$$\begin{aligned}&\rho\frac{\partial u}{\partial t}+\rho\left(u\cdot\nabla\right)u\\&=\nabla\cdot\left[-p+\mu\left(\nabla u+\left(\nabla u\right)^T\right)-\frac{2}{3}\mu\left(\nabla\cdot u\right)\right]+F+\rho g\end{aligned} \tag{10}$$

$$\rho c_p\frac{\partial T}{\partial t}+\rho c_p u\cdot\nabla T=\nabla\cdot\left(k\nabla T\right)+Q \tag{11}$$

where u is the gas velocity vector, F is the volume force, g is the gravitational acceleration constant, and Q is the heat source, including the Joule heat losses in both the conductor and the enclosure. In addition, ρ, p, μ, c_p and k are the density, pressure, kinetic viscosity, specific heat at constant pressure and thermal conductivity of the mixed gas or the air.

In this paper, the atmospheric temperature remains constant at infinity, and the temperature is not affected by the GIL. Therefore, the boundary temperature conforms to the first kind of boundary condition, which is given by

$$T=T_i \tag{12}$$

where T_i is the initial temperature of the environment.

The convective heat transfer boundary conditions on the outer surface of the enclosure and the surface of the conductor are stated as follows:

$$-k\frac{\partial T}{\partial n}=h_a\left(T_e-T_a\right) \tag{13}$$

$$-k\frac{\partial T}{\partial n}=h_b\left(T_c-T_g\right) \tag{14}$$

where T_e is the enclosure temperature, T_a is the ambient temperature, and T_c and T_g are the conductor temperature and the temperature of the insulating gas, respectively. h_a is the heat transfer coefficient between the enclosure and the air. h_b is the heat transfer coefficient between the conductor and the insulating gas.

The radiation heat transfer process at the interface between the outer surface of the enclosure and the air is set as a boundary condition, which can be expressed as follows:

$$-k\frac{\partial T}{\partial n}=\varepsilon_{e0}\sigma\left(T_e^4-T_a^4\right) \tag{15}$$

where n is the length of the outer boundary surface in the normal direction, ε_{eo} is the outer surface emissivity, and σ is the Stefan-Boltzmann constant.

Similarly, only the radiation heat transfer process at the interface between the conductor and the Fluoronitriles-CO_2 gas mixture is considered, and its boundary condition is given as follows [15].

$$-k\frac{\partial T}{\partial n}=\frac{\sigma\left(T_c^4-T_e^4\right)}{\dfrac{1}{\varepsilon_{c0}}+\dfrac{D_{c0}}{D_{ei}}\left(\dfrac{1}{\varepsilon_{ei}}-1\right)} \tag{16}$$

where ε_{ei} and ε_{c0} are the emissivities of the inner surface of the enclosure and the outer surface of the conductor, respectively, and D_{c0} and D_{ei} are the outer diameter of the conductor and the inner diameter of the enclosure, respectively.

2.3 Model verification

The finite element numerical calculation process is performed as follows. First, the resistivity values of the conductor and the enclosure are calculated using the formula for the resistivity change with temperature, where the two material types are aluminum and aluminum alloy. Then, the Joule heat loss of the conductor and the enclosure under the rated current is calculated. The loss, which acts as a heat source, is coupled to the analysis of the fluid-temperature coupled field. The solution for the temperatures of the conductor and the enclosure is compared with the initial temperature. In this way, the GIL temperature distribution in the stable state can finally be obtained.

It is assumed that the ambient temperature of the simulation is 293.15 K and that the load current is 2000 A. The GIL cavity is filled with the Fluoronitriles-CO_2 gas mixture, where the gas mixture pressure is 0.3 MPa. The temperature distribution of the GIL in the steady state is shown in Fig. 2. The figure shows that the temperature distributions of the conductor and the enclosure all presented a specific gradient distribution state. The highest temperature was 353.8 K, which occurred at the top of the conductor, and the temperature difference between the top and the bottom of the conductor was 1.2 K. In addition, the temperature difference between the interior and exterior of the hollow conductor was approximately 0.3 K.

To verify the proposed analytical model, a temperature rise experiment was performed. The temperature rise test platform of the GIL is as shown in Fig. 3. The test platform was mainly composed of a practical GIL pipeline, a HYDDN-200/10000A large current generator, a data acquisition system and a set number of temperature sensors. The large current generator has a rated input capacity of 200 kVA with a rated input frequency of 50 Hz. The rated input voltage is 380 V. The rated input current is 500 A, while the rated output current is 10 kA. The cooling method used is dry self-cooling. The generator can run continuously for long periods at 100% rated voltage and current and can thus satisfy the requirements of the temperature rise experiment. The temperature information collected by the sensors are transmitted to the data management platform through the wireless transmitting device. And the sensors used in the temperature acquisition system is PT1000 with a precision of 0.1K. The sensors are arranged on the top, middle and bottom parts of the conductor, the enclosure, and in the gas environment, respectively. The location of the sensors in the gas environment are at the middle point between the conductor and the enclosure. To ensure good contact between the temperature sensors and test points, thermal conductive silica gel is coated on the contact surface.

The experiment was performed indoors, thus allowing the effects of wind speed and solar radiation on the experimental results to be avoided. The temperature difference at room temperature was measured to be less than 0.4 K using a thermometer. The output current from the large current generator was adjusted until the number remained stable and the temperature distribution of the GIL was obtained

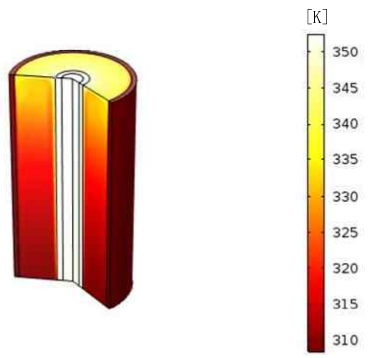

Fig. 2. Temperature distribution of the AC GIL

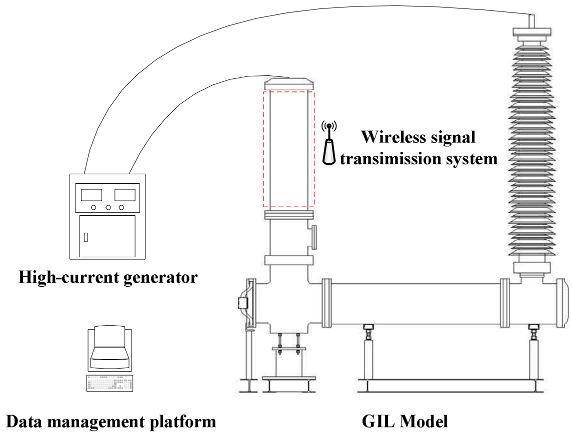

Fig. 3. Temperature rise test platform for the GIL

Table 2. Temperature rise results from FEM and experiments

Temperature rise(K)	Method	Top	Middle	Bottom
Conductor	FEM Experiment	60.7 61.5	60.2 61.1	59.6 59.9
Gas	FEM Experiment	38.3 37.4	29.1 28.5	21.9 23.6
Enclosure	FEM Experiment	16.8 17.9	16.1 15.7	15.7 14.8

after the temperature rise experiment was performed for 10 h. The stability criterion used in the experiment was that the temperature change curves of each of the temperature measurement points must tend towards a plane, and the temperature change at each temperature measurement point in a 10 min period must be less than 0.1 K. To ensure the accuracy of the experiment, repeated measurements were carried out under various working conditions. The load current was varied by adjusting the output current from the large current generator.

Both the simulations and the experiments were performed under a rated load condition of 2000 A. The temperature rise values of the conductor and the enclosure that were obtained from the finite element simulations and the temperature rise experiments are listed in Table 2. The results in Table 2 show that the temperature rises at the measurement points in the conductor, the enclosure and the gas obtained from the simulations match the experimental results well. Therefore, it can be concluded that the finite element simulation method used in this work is reliable. The model can also be used to calculate and analyze the temperature rise characteristics of a GIL operating under high pressure or with a high ratio gas mixture, which cannot be obtained easily via experiments.

3. Results

The finite element model was used to study the temperature distribution of the GIL when filled with the Fluoronitriles-CO_2 gas mixture. To be as close to the actual operating conditions as possible, the GIL filled with the Fluoronitriles-CO_2 mixture was set to operate at 2000 A (the rated load current) at a pressure of 0.7 MPa. The steady state distributions of the temperature and the gas flow velocity in GIL are shown in Fig. 4. In Fig. 4(a), the temperature distributions of the conductor and the enclosure both present specific gradient distributions. The highest temperature, which is 348.2 K, occurs at the top of the conductor. The temperature difference between the top and the bottom of the conductor is 1.4 K. The highest temperature of the enclosure, which is 309.9 K, also appears in the upper part. In addition, the temperature difference between the inner and outer surfaces of the enclosure is approximately 1 K. Comparison of the temperature distribution and the gas flow vector diagram

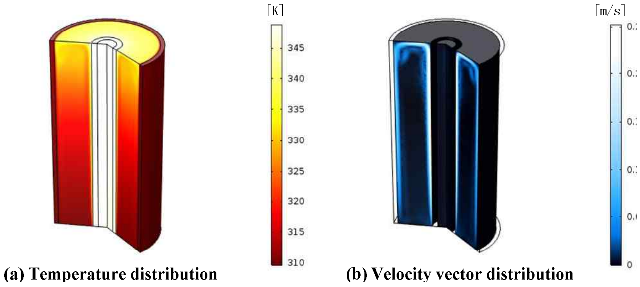

(a) Temperature distribution **(b) Velocity vector distribution**

Fig. 4. Temperature and gas flow velocity distributions of the GIL under steady state conditions

shows that because of gravity, buoyancy effects and uneven heating of the gas, the GIL conductor, enclosure and gas all showed distribution characteristics in which the temperature in the upper part of each structure is higher than that in the lower part. This indicated that convection heat transfer played a dominant role in the heat transfer processes of the GIL and that the change of gas properties would affect the temperature distribution of the GIL directly.

The temperature distributions of GILs that were filled with CO_2, SF_6 and the Fluoronitriles-CO_2 mixture were simulated and compared. The temperature distributions of the GILs when filled with the three types of gas are shown in Fig. 5. The results in Fig. 5 show that the temperature rise of the conductor in the GIL that was filled with the Fluoronitriles-CO_2 mixture was lower than that of the GIL filled with CO_2 gas under the same conditions. The results showed that the addition of a small amount of the Fluoronitriles gas provided a specific improvement in the heat transfer performance of the GIL. This phenomenon is mainly caused by two important physical parameters of gas convection heat transfer: the dynamic viscosity and the constant pressure heat capacity. For these two gas types, the dynamic viscosity of the Fluoronitriles gas is smaller than that of CO_2, and its constant pressure heat capacity is higher than that of CO_2. The heat dissipation of the Fluoronitriles-CO_2 gas mixture is lower than that of the SF_6 gas. The temperature differences between the conductors ranged from 7 K to 8 K when the GILs were filled with SF_6 and Fluoronitriles-CO_2 mixture respectively. Temperature rise differences in this range can be compensated using typical measures, such as addition of cooling fins to the enclosure or addition of machined slots and holes to the conductor to improve the convection around the GIL's charged parts [5]. With regard to the temperature rise of the enclosure, the differences among the three types of gases were relatively small. However, with regard to the selection of the alternative insulating gas for use in the GIL, it is necessary to ensure that the GIL operates at a suitable temperature. Using a process of comparison and analysis, we see that the gas substitution scheme that used the Fluoronitriles and a buffer gas has a thermodynamic foundation and shows particular application potential.

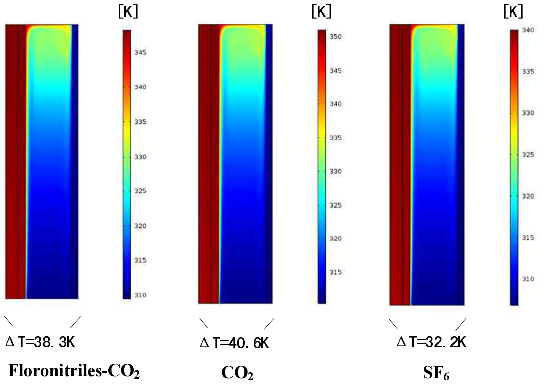

Fig. 5. Temperature distributions of GILs filled with the Fluoronitriles-CO_2 mixture, CO_2, and SF_6

3.1 Effects of the proportions of the gas components

Because the 4% Fluoronitriles-96% CO_2 gas mixture shows obvious differences to pure CO_2, it is necessary to analyze the effects of the proportions of gas components. In this section, the applied operating current is 2000 A and the pressure inside the GIL remains at 0.7 MPa. When the insulation property and liquefaction temperature are considered according to [20] and [21], 20%Fluoronitriles-80%CO_2 reaches the same dielectric performance with pure SF_6 at 0.1MPa. And the 3.7 % Fluoronitriles - 96.3% CO_2 mixture provides a good compromise and an appropriate substitute mixture for SF_6 gas for high voltage apparatus under a low temperature. Therefore, the ratios of the Fluoronitriles contained in the Fluoronitriles-CO_2 mixtures are selected to be 0%, 4%, 8%, 12%, 16%, and 20%, respectively. The temperature rises in the GIL conductors and enclosures are as shown in Fig. 6.

The line graph shows that the temperature rise in the GIL decreases as the proportion of Fluoronitriles gas increases. When a small amount of the Fluoronitriles gas was mixed into the CO_2, the temperature rise could be reduced significantly, but as the increase in the proportion of the Fluoronitriles gas increases, the downward trend of the demonstrated by the conductor slowed down slightly. However, the temperature rise in the enclosure was not obvious and it only increased slightly with increasing Fluoronitriles proportion. This occurs because when the current and the pressure are fixed, the temperature rise in the GIL enclosure is largely determined by the enclosure geometry and the initial temperature of the ambient air. Within a specified range, the effects of the proportions of the mixture are relatively small.

3.2 Effects of gas pressure

To choose the most appropriate gas pressure of Fluoronitriles-CO_2 gas mixture, dielectric breakdown properties should be considered first. According to [20], in homogeneous and quasi-homogeneous field, equivalences to 0.55 MPa SF_6 is obtained with 3.7% Fluoronitriles-

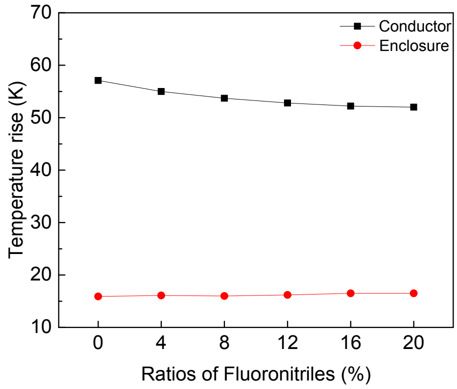

Fig. 6. Relationship between the temperature rise of the GIL and the proportion of Fluoronitriles gas used

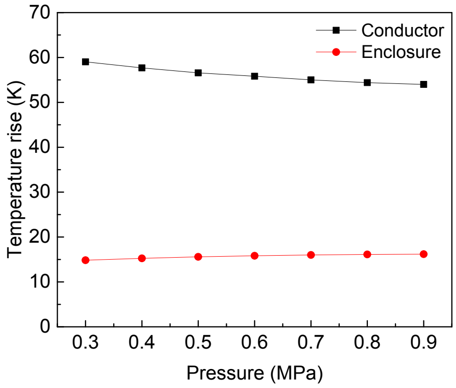

Fig. 7. Relationship between gas pressure and GIL temperature rise

96.3% CO_2 mixtures at 0.88 total pressure. Based on the reference and the SF_6 equipment in actual, the total pressure of the 4% Fluoronitriles-96% CO_2 mixture are selected ranging from 0.3 MPa to 0.9 MPa. The effects of the gas pressure on the temperature rise in the GIL conductor and enclosure are as shown in Fig. 7. The conductor current is under 2000 A, as well. And the simulation results showed that the temperature of the GIL conductor actually decreased with increasing pressure, while the enclosure temperature increased slightly. This occurs because when the gas pressure inside the GIL rises, the density of the gas also increases. Therefore, the heat capacity of the gas per unit volume increases, and the heat that is transferred by convection also increases. As a result, the temperature of the GIL conductor decreases while the temperature of the enclosure rises. However, the effects of pressure on the heat transfer processes of the gas are limited. With further increases in pressure, the increase in the gas heat transfer slows down.

4. Analysis on Current-Carrying Capacity

The heat transfer performance of the insulating gas will influence the design of the current-carrying capacity of the

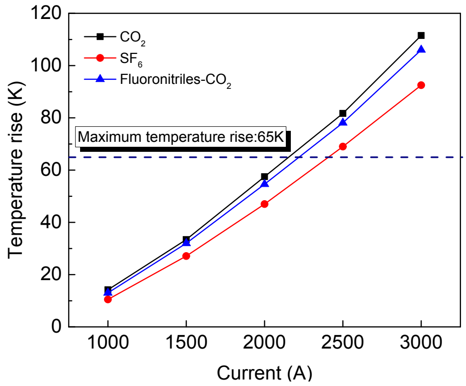

Fig. 8. Relationship between load current and the temperature rise in the GIL conductor

environmentally-friendly GIL. In this section, under the assumption that the ambient temperature is 293.15 K, the temperature rises in the GIL conductor under different load currents are as shown in Fig. 8. It is known from the simulation results that the temperature of the GIL increases in a nonlinear manner with increasing load current. Therefore, in the design and application of the GIL, the appropriate rated current must be selected first; otherwise the service life of the GIL will be seriously affected. According to [22], the maximum allowable temperature rise in the GIL conductor is 65 K. Therefore, this upper limit for the temperature rise was used to calculate the current-carrying capacities of the GILs with the three types of gases. The calculation results indicated that the current-carrying capacity of the central conductor of the GIL that was filled with the Fluoronitriles-CO_2 gas mixture was 2223 A, while that capacity of the GIL filled with SF_6 gas was 2408 A, and that of the GIL filled with CO_2 gas was 2155 A. It can thus be concluded that under the same structure and pressure conditions, when the new type of insulating gas is applies to the GIL, its current-carrying capacity is reduced to a certain extent when compared with SF_6. To enable the design of an environment-friendly GIL, the current-carrying capacity must be optimized.

When the temperature rise in the conductor reaches the upper limit of 65 K under the same external conditions, the relationship among the gas pressure, the ratio of the gas mixture components and the maximum current-carrying capacity of the conductor is as shown in Fig. 9. The chart shows that under the conditions where the liquefaction temperature and insulation strength of the gas are satisfactory, increasing the gas pressure and/or the mixing ratio of the Fluoronitriles in the gas mixture appropriately will enhance the current-carrying capacity of the GIL. Therefore, the chart can be used for reference in the design of GIL current-carrying capacity.

There is a major difference between the AC GIL and the DC GIL in terms of the heat source. According to the principle of electromagnetic induction, in addition to the current in the conductor, an equal and opposite current must be induced in the enclosure by the source current.

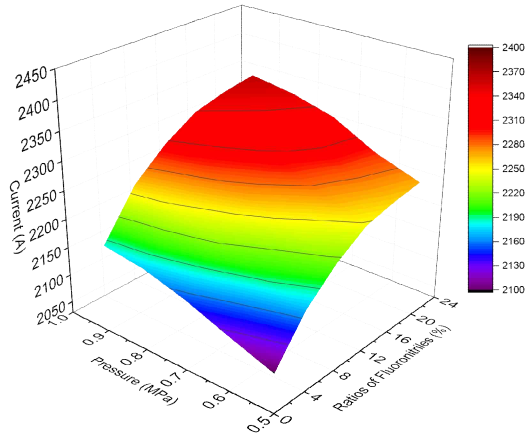

Fig. 9. Relationship among the current-carrying capacity of the GIL conductors, the gas pressure and the ratio of the Fluoronitriles

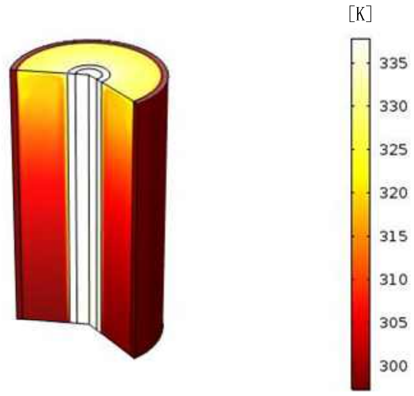

Fig. 10. Temperature distribution of DC GIL filled with Fluoronitriles-CO_2 mixture

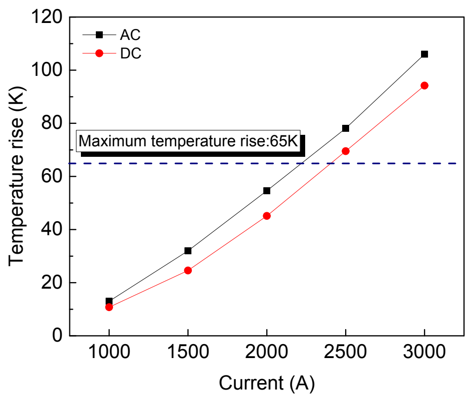

Fig. 11. Comparison of temperature rises of AC-GIL and DC-GIL conductors with variation of the load current

Therefore, the current in the conductor tends towards the skin, while the current in the enclosure tends inward towards the skin. Unlike the AC GIL, when the current passes through the internal conductor in the DC GIL, no skin effect occurs. Therefore, the equivalent resistance of the DC GIL decreases. In addition, no eddy current is induced in the enclosure. As a result, the Joule heating loss in the DC GIL is concentrated on the central conductor.

Based on the above analysis, a DC GIL model operating at 2000 A and filled with the Fluoronitriles-CO_2 mixture at 0.7 MPa was established. The steady state temperature distribution of this model is shown in Fig. 10. From this figure, it was observed that the temperature distribution over the entire area was a two-dimensional axisymmetric distribution, and both the conductor and the enclosure were shown to have gradient distributions. Under the same conditions, the temperature rises in both the conductor and the enclosure were lower than those of the AC GIL. Additionally, because eddy currents do not exist in the DC GIL enclosure, the conductor is the only heat source. Therefore, the temperature rise was relatively small. In the GIL filled with the Fluoronitriles-CO_2 gas mixture, when the conductor reaches the highest temperature rise of 65 K, its current-carrying capacity reaches 2405 A. When compared with the AC GIL, the current-carrying capacity of the DC GIL has improved significantly. The curve is shown in Fig. 11, which depicts the conductor temperature rise with changes in the load current in both the AC GIL and the DC GIL.

5. Conclusion

1) In the finite element calculations, the physical parameters of the mixed gas are obtained using the theory of multiple species transport. In addition, a compressible laminar flow model at low Mach number is used to improve the calculation accuracy and ensure that the flow and heat transfer behavior of the gas mixture are closer to the real conditions. The calculation model was verified experimentally, thus demonstrating the validity and reliability of the proposed method.

2) The temperature distribution of the vertically installed GIL filled with the Fluoronitriles-CO_2 mixture shows gradient distribution characteristics in which the temperature of the upper part is higher than that of the lower part. The heat transfer performance of the Fluoronitriles-CO_2 gas mixture is not as good as that of SF_6 gas, but it is superior to that of CO_2 gas. Addition of a small amount of Fluoronitriles improves the heat dissipation capacity of the insulating gas and shows good heat transfer performance. This provides the thermodynamic basis and potential for application of these GILs to high-capacity electricity transmission. The temperature rise of the GIL decreases as the component proportion of the Fluoronitriles gas in the mixture increases, and decreases with increasing insulating gas pressure. Under the premise that the GIL's mechanical strength and insulation gas liquefaction temperature are appropriate, the temperature rise performance of the GIL can be improved by increasing the mixing ratio of the Fluoronitriles gas and/or increasing the gas pressure of the GIL.

3) When compared with the GIL that is filled with SF6, the current-carrying capacity of the GIL will be reduced if the Fluoronitriles-CO_2 mixture is used as a substitute insulating gas. Therefore, when designing the current-carrying capacity of the GIL that is to be filled with the Fluoronitriles-CO_2 gas mixture, the heat transfer performance of this new type of insulating gas must also be considered. If the gas insulation performance and liquefaction temperature conditions are satisfied, increasing the gas pressure, increasing the Fluoronitriles ratio, and/or optimizing the GIL structure can improve its heat dissipation capacity. In addition, the DC GIL has a higher current capacity than the AC GIL when using the same structure and it offers a good solution for high-capacity energy transmission.

Acknowledgements

This work was supported by the National Key R&D Program of China (2017YFB0902500) and the Fundamental Research Funds for the Central Universities (2018MS005). The authors are also grateful to 3M^{TM} Company for providing Novec^{TM}4710 gas and technical support in this research. In addition, The authors would like to thank Dr. Zhikang Yuan for his valuable advice on this research.

References

[1] H. Koch, *Gas-insulated Transmission Lines (GIL)*. USA: A John Wiley & Sons, Ltd. 2012, pp. 1-5.

[2] J. L. He, "Ideas on building underground energy complex passage," *Southern Power System Technology*, vol. 10, no. 3, pp. 66-70, Mar. 2016. (in Chinese)

[3] M. Khalifaed, *High Voltage Engineering*. New York: Marcel Dekker, Inc., 1990.

[4] H. Sadakuni, K. Sasamori, H. Hama, and K. Inami, "Insulation and current carrying design for GIS," *Japan Inst. Elec. Eng*., vol. 9, pp. 33-42, Mar. 1996.

[5] Y. Kieffel, A. Girodet, F. Biquez, Ph. Ponchon, J. Owens, M. Costello, M. Bulinski, R. Van San, K. Werner, "SF6 alternative development for high voltage switchgear," in *Electrical Insulation Conference*, 2015, pp. 379-383.

[6] Y. Kieffel, Todd Irwin, Ph. Ponchon, J. Owens, "Green gas to replace SF6 in electrical grids," *IEEE Power Energy Mag*., vol. 14, pp. 32-39, Apr. 2016.

[7] D. Gautschi, A. Ficheux, M. Walter, J. Vuachet, "Application of a fluoronitrile gas in GIS and GIL as an environmental friendly alternative to SF6," in *CIGRE*, 2016, pp. 1-11.

[8] M. Ghassemi, M. Farzaneh. "Coupled computational fluid dynamics and heat transfer modeling of the effects of wind speed and direction on temperature

increase of an ice-covered FRP live-line tool," *IEEE Trans. Power Del.*, vol. 30, no. 5, pp. 2268-2275, Oct. 2015.
[9] M. T. Dhotre, J. Korbel, X. Ye, J. Ostrowski, S. Kotilainen and M. Kriegel. "CFD simulation of temperature rise in high-voltage circuit breakers", *IEEE Trans. Power Del.*, vol. 32, no. 6, pp. 2530-2536, Dec. 2017.
[10] D. Minaguchi, M. Ginno, K. Itaka, et al. "Heat transfer characteristics of gas-insulated transmission lines," *IEEE Trans. Power Del.*, vol. 1, no. 1, pp. 1-9, Jan. 1986.
[11] H. Koch, A. Chakir, "Thermal calculationa for buried gas-insulated transmission lines (GIL) and XLPE-Cable," in *Power Engineering Society Winter Meeting*, 2001, pp. 857-862.
[12] R. Benato, F. Dughiero, "Solution of coupled electro-magnetic and thermal problems in gas-insulated transmission Lines," *IEEE Trans. Magn.*, vol. 39, no. 3, pp. 1741-1744, May. 2003.
[13] J. K. Kim, S. C. Hahn, K Y Park, H. K. Kim, Y. H. Oh, "Temprature rise prediction of EHV GIS bus bar by coupled magnetothermal finite element method," *IEEE Trans. Magn.*, vol. 41, no. 5, pp. 1636-1639, May. 2005.
[14] X. W. Wu, N. Q. Shu, L. Li, H. T. Li, H. Peng, "Finite element analysis of thermal problems in gas-insulated power apparatus with multiple species transport techniques," *IEEE Trans. Magn.*, vol. 50, no. 2, pp. 321-324, Feb. 2014.
[15] B. Li, D. M. Xiao, S. Zhao, H. Zhang, "Temperature rise numerical calculation of the second generation gas insulated transmission line," *Transaction of China Electrotechnical Society*, vol. 32, no. 13, pp. 272-276, Jul. 2017. (in Chinese)
[16] W. D. Bennon and F. P. Incropera, "A continuum model for momentum, heat and species transport in binary solid-liquid phase change systems-I. Model formulation," *Int. J. Heat Mass Trans.*, vol. 30, no. 10, pp. 2161-2170, Oct. 1987.
[17] J. D. Anderson, *Computational Fluid Dynamics: The Basics with Applications*, New York: Mc Graw-Hill, 1995, pp. 452-455.
[18] Z. N. Zhao. *Heat transfer theory*. Beijing: Higher Education Press, 2008, pp. 177-179. (in Chinese)
[19] L. J. Wu. *Theoretical basis and design of large current bus-bars*, Beijing: Water Conservancy and Hydropower Press, 1985, pp. 246-253, 1985 (in Chinese).
[20] H. E. Nechmi, A. Beroual, A. Girodet, P. Vinson, "Fluoronitriles/CO_2 gas mixture as promising substitute to SF_6 for insulation in high voltage applications," *IEEE. Trans. Dieletr. Electr. Insul.*, vol. 25, no. 5, pp. 2587-2593, Oct. 2016.
[21] 3M USA SDS, 3M™ Novec™ 4710 Dielectric Fluid, 33-6330-6, Version 2.03, 2015-02-04.
[22] Common technical requirements for high-voltage switchgear and control equipment standards, GB/T 11022-2011, 2011-12-30 (in Chinese).
[23] T. Magier, M. Tenzer, H. Koch. "Direct current gas-insulated transmission lines," *IEEE Trans. Power Del.*, vol 33, no. 1, pp. 440-446, Feb. 2018.

Geng Chen was born in Baoding, Hebei Province, China, in 1990. Currently, he is a Ph.D. candidate in North China Electric Power University, Beijing, China. His research interests include characterization of alternative gases for high voltage insulation and surface charge behavior, material modification for dielectrics in GIS/GIL.

Youping Tu was born in Ningbo, Zhejiang, China, in 1966. She received her B.Sc. and M.Sc. degrees from the Department of Electrical Engineering, Chongqing University in Chongqing, China, respectively in 1988, and in 1991. Currently, she is a professor in the Department of Electrical Engineering at North China Electric Power University in Beijing, China. From 1991 to 1994, she worked in the computer application field in Hangzhou Heat Power Plant, Zhejiang Province, China. During 1994, she was a research assistant in the Department of Precision Instrument and Mechanics, Tsinghua University in Beijing, China. From 1994 to 1995, she worked in Ludao Company in Beijing, China. She was a lecturer from 1995 to 2003, and an associate professor from 2004 to 2010 in the Department of Electrical Engineering at North China Electric Power University in Beijing, China. Her research interest includes insulation technology, overvoltage and protection for power system. She is the author of more than 100 technical papers.

Cong Wang was born in Ganzhou, Jiangxi Province, China, in 1980. He obtained his B.Sc. and M.Sc. degrees from the Department of Electrical Engineering, North China Electric Power University in Beijing, China, respectively in 2002, and in 2012. Currently, he is an Engineer in the Department of Electrical Engineering, North China Electric Power University in Beijing, China. His research interests include properties of the dielectric material, gas discharge and online monitoring of electrical equipment.

Yi Cheng was born in Jingdezhen, Jiangxi Province, China, in 1994. He received the B.Sc. degree in electrical engineering from Changshu Institue of Science and Technology, Suzhou, in 2015. Currently, he is a Master Degree Candidate in electrical engineering at North China Electric Power University. His research interests include include properties of the dielectric material, gas discharge and online monitoring of electrical equipment.

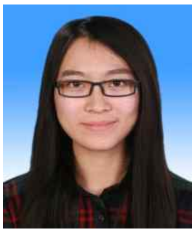

Han Jiang was born in Baoding, Hebei Province, China, in 1994. She received the B. Sc. degree in electrical engineering from North China Electric Power University, Beijing, in 2016. Currently, she is a M.Sc. candidate in electrical engineering at North China Electric Power University. Her research interests include electrical insulation materials and high voltage engineering.

Hongyang Zhou was born in Fujian province, China, in 1991. He received the B.S. degree in electrical engineering from North China Electric Power University, Beijing, in 2014. He is now working for Ph.D. degree in electrical engineering in North China Electric Power University, Beijing, China. His research interests include electrical insulation materials and online monitoring of electrical equipment.

Hua Jin was born in Hailin, Heilongjiang Province, China, in 1971. She obtained her B.Sc degree of computer science and M.Sc. degree of electrical engineering theory and new technology from Harbin University of Science and Technology, Harbin, China, respectively in 1994, and in 2000. Currently, she is an associate professor of the school of control and computer Engineering, North China Electric Power University in Beijing, China. Her research interests include data analysis and deconstruction, big data applications, etc.